

Spectropolarimetry of the Type Ib/c SN 2005bf*

Justyn R. Maund¹†, J. Craig Wheeler¹, Ferdinando Patat², Dietrich Baade²,
Lifan Wang³, and Peter Höflich⁴

¹ Department of Astronomy and McDonald Observatory, 1 University Station C1400, University of Texas, Austin, Texas, 78712, U.S.A.

² ESO - European Organisation for Astronomical Research in the Southern Hemisphere, Karl-Schwarzschild-Str. 2, 85748 Garching
b. München, Germany

³ Department of Physics, Texas A&M University, College Station, Texas 77843-4242, U.S.A.

⁴ Department of Physics, Florida State University, Tallahassee, Florida 32306-4350, U.S.A.

12 November 2018

ABSTRACT

We present spectropolarimetric observations of the peculiar Type Ib/c SN 2005bf, in MCG+00-27-005, from 3600-8550Å. The SN was observed on 2005 April 30.9, 18 days after the first B-band light-curve maximum and 6 days before the second B-band light-curve maximum. The degree of the Interstellar Polarization, determined from depolarized emission lines in the spectrum, is found to be large with $p_{max}(ISP) = 1.6\%$ and $\theta(ISP) = 149.7 \pm 4.0$, but this may be an upper limit on the real value of the ISP. After ISP subtraction, significant polarization is observed over large wavelength regions, indicating a significant degree of global asymmetry, $\gtrsim 10\%$. Polarizations of 3.5% and 4% are observed for absorption components of Ca II H&K and IR triplet, and 1.3% for He I 5876Å and Fe II. On the $Q - U$ plane clear velocity-dependent loop structure is observed for the He I 5876Å line, suggestive of departures from an axial symmetry and possible clumping of the SN ejecta. Weak High Velocity components of H α , H β and H γ are observed, with velocities of $-15\ 000\text{km s}^{-1}$. The low degree of polarization observed at H β suggests that the polarization observed for the other Balmer lines ($\sim 0.4\%$ above the background polarization) may rather be due to blending of H α and H γ with polarized Si II and Fe II lines, respectively. We suggest a model in which a jet of material, that is rich in ^{56}Ni , has penetrated the C-O core, but not the He mantle. The jet axis is tilted with respect to the axis of the photosphere. This accounts for the lack of significant polarization of O I 7774Å, the delayed excitation and, hence, observability of He I and, potentially, the varied geometries of He and Ca.

Key words: supernovae:general – supernovae:individual:2005bf – techniques:spectroscopic – techniques:polarimetric

1 INTRODUCTION

The presence of asymmetries in core-collapse supernovae (CCSNe) has long been thought inherent to the nature of the explosion mechanism. The history of observations of run-away O-stars and pulsars gave the first direct evidence for such asymmetries (Dray et al. 2005). Studies of the profiles of emission lines in the late-time SNe spectra (Mazzali et al. 2005) and the morphologies of young remnants (Fesen et al. 2006) also provided important clues. The link between the SNe and the highly-collimated Gamma Ray Burst (GRB)

phenomenon (Woosley & Bloom 2006), along with studies of the spherical nature of Type IIP SNe for their use as distance indicators (Hamuy & Pinto 2002; Leonard et al. 2001), has necessitated direct studies of SN asymmetries at all stages of their evolution.

Spectropolarimetry, along with the new era of 8m-class telescopes, has permitted the routine observation of CCSNe, inferring the asymmetries directly from the polarization properties of these SNe. While other techniques, such as the modelling of emission line profiles, probe the interaction between the SN ejecta and the circumstellar medium (CSM), only spectropolarimetry provides a direct measure of the geometries of SN ejecta and, more importantly at earlier epochs, the nature of the geometry of the core-collapse mechanism itself. The linear polarization of light, induced by electron

* Based on observations made with ESO Telescopes at the Paranal Observatory, under programme 75.D-0213.

† Email: jrm@astro.as.utexas.edu

and line scattering, in spherically symmetric atmospheres are completely cancelled, leading to no net observed linear polarization. In the presence of irregularities or asymmetries, a net linear polarization is observed, with the magnitude of the polarization and the polarization angle related to the relative size of the asymmetry and the orientation of the asymmetry on the sky (Shapiro & Sutherland 1982; McCall 1984; Höflich 1991).

CCSNe are generally classified by the absence (Type I) or presence (Type II) of hydrogen in their early spectra (Filippenko 1997). Type I CCSNe are generally observed to have higher degrees of polarization, suggesting higher degrees of asymmetries, than for Type II CCSNe at early times. This is inferred as the direct observation of the core layers in Type I SNe, which are shielded by the hydrogen ejecta in Type II SNe (Wang et al. 2001; Leonard et al. 2006). Once the hydrogen layers of Type II SNe become optically thin, revealing the inner core layers, the polarization is observed to increase dramatically (see SN 2004dj, Leonard et al. 2006; SN 2001ig, Maund et al. 2007). Observations of the Type Ic SN 2002ap, which was considered a possible host for a GRB misaligned with the line of sight, showed it to have polarizations of $\gtrsim 1\%$, corresponding to asymmetries of $\sim 20\%$ (Leonard et al. 2002; Wang et al. 2003). Additionally, the orientation of the observed polarization, through studies of the Stokes Q and U parameters, showed that O and Fe had different distributions within the SN ejecta (Wang et al. 2003).

SN 2005bf was discovered independently by Monard and the team of Li and Moore (Monard et al. 2005) on 2005 Apr 6.72 UT. Li and Moore determined the position of SN 2005bf as $\alpha_{2000} = 10^{\text{h}}23^{\text{m}}57.27^{\text{s}}$ and $\delta_{2000} = -3^{\circ}11'28.6''$, $11.7''$ east and $32.6''$ south of the nucleus of the host galaxy MCG+00-27-005 (see Fig. 1). The heliocentric recessional velocity of the host is given by HyperLEDA¹ as $v_{\odot} = 5655\text{km s}^{-1}$, with the recessional velocity corrected for infall to Virgo, $v_{\text{vir}} = 5623\text{km s}^{-1}$, yielding a distance of 75Mpc (for $H_0 = 75\text{km s}^{-1}\text{Mpc}^{-1}$).

SN 2005bf was a peculiar Type Ib/c SN. It showed a double-peaked light curve with a first maximum at ~ 16 days post-explosion and a second, brighter maximum at ~ 40 days post-explosion (Folatelli et al. 2006), assuming an explosion date of 2005 March 28 (Tominaga et al. 2005). At early epochs little or no He was observed, giving some resemblance to a Type Ic SN (Morrell et al. 2005; Modjaz et al. 2005). By the second maximum, He I was observed in the spectrum (Wang & Baade 2005), giving the appearance of a Type Ib SN (Tominaga et al. 2005; Folatelli et al. 2006). Tominaga et al. (2005) and Folatelli et al. (2006) invoke “jets” and “holes” to explain the observed behaviour. If either behaviour is involved, one would expect strong asymmetries to be revealed by spectropolarimetry (Wang et al. 2001).

Here we present spectropolarimetry of SN 2005bf to elucidate the nature of the explosion. We find that neither published model accounts for the spectropolarimetry and suggest a new configuration that may better account for the observations. The observation of SN 2005bf is presented in Section 2, with the results of these observations presented

Figure 1. FORS1 1s V-band image of the location of SN 2005bf, relative to its host galaxy MCG+00-27-005. The SN is indicated by the cross-hairs, and the arrow indicates the direction of the ISP determined in Section 4.1.

in §3. In §4 these results are analysed, and they are subsequently discussed in §5.

2 OBSERVATIONS

SN 2005bf was observed on 2005 Apr 30.9 (all times are UT), using the European Southern Observatory (ESO) Very Large Telescope (VLT) Kueyen Telescope with the Focal Reducer and Low Dispersion Spectrograph 1 (FORS1) instrument in the spectropolarimetric PMOS mode (Appenzeller et al. 1998). These observations are summarised in Table 1. The FORS1 instrument was used with the standard resolution collimator, providing a plate scale of $0.2''\text{px}^{-1}$. The standard “striped” PMOS slit mask was used, with slit width $1''$ and length $22''$, and throughout the entire set of observations the slits were kept at a position angle $\text{PA} = 0^{\circ}$. Observations of SN 2005bf were conducted with the “super achromatic” retarder plate positioned at 4 angles: 0° , 45° , 22.5° and 67.5° . The two beams, at each retarder plate position, were dispersed using the G300V grism, which provides a dispersion of $2.6\text{\AA}\text{px}^{-1}$ and spectral resolution, measured from arc lamp calibration exposures, of 12.3\AA . In this instance an order separation filter was not used leading to some additional flux contamination at $\lambda \gtrsim 7000\text{\AA}$. The total wavelength coverage of the data was $\sim 3600 - 8550\text{\AA}$. FORS1 uses a 2048×2048 Tektronix CCD detector, and the observations were conducted with gain $0.71e^{-}\text{ADU}^{-1}$, with a readout noise of $5.6e^{-}$. The data were reduced in the standard manner using IRAF² and a series of our own routines, written in the Perl Data Language³. The data were corrected for bias and overscan. A master unpolarized normalised flat was constructed from flat observations acquired with the retarder plate at each of the four angles. The flat was applied to object frames, and object spectra, for the ordinary and extraordinary rays at each of the four retarder plate angles, were optimally extracted. These spectra were wavelength calibrated through comparison with observations of HeHgArCd arc lamps. The Stokes parameters Q and U , the total polarization p and the polarization angle θ were calculated in the standard manner (see Jehin et al. 2005), with the data re-binned to 15\AA to improve the signal-to-noise (S/N) for the individual Stokes parameters. A correction was applied for the wavelength-dependent chromatic zero angle offset.

The spectropolarimetric calibration of the FORS1 instrument was checked by observing, with 30s exposures at each retarder plate angle, the spectropolarimetric standard Vela195, on 2005 Apr 30.98. These data were reduced in the same

¹ <http://leda.univ-lyon1.fr/>

² IRAF is distributed by the National Optical Astronomy Observatories, which are operated by the Association of Universities for Research in Astronomy, Inc., under cooperative agreement with the National Science Foundation - <http://iraf.noao.edu/>

³ <http://pdl.perl.org/>

Table 1. Spectropolarimetric ESO VLT FORS1 observations of SN 2005bf on 2005 Apr 30/May 1

Object	Avg. Airmass	Retarder Plate Angles	Exp. time (s)
Vela 1 95 ¹	1.09	0,45,22.5, 67.5	4 × 30
SN 2005bf	1.13	0,45,22.5, 67.5	4 × 2 × 1200
GD153 ²	1.46	0	300

¹ Polarized Standard² Flux Standard

manner and found to be consistent with previous measurements. A single 300s observation of GD 153, with full polarimetry optics and the retarder plate at 0°0, was used to provide a flux calibration and facilitate the removal of telluric features from the observations of SN 2005bf. At each retarder plate angle the average spectrum wide S/N \sim 250. The data were corrected for the heliocentric recessional velocity of the host galaxy. Statistical uncertainties of the measured Stokes parameters were estimated using a Monte Carlo simulation of the FORS1 instruments, in a similar style to the model of Patat & Romaniello (2006).

3 OBSERVATIONAL RESULTS

The spectropolarimetric properties of SN 2005bf are shown as Fig. 2. The epoch of the observations (JD2453492.5) corresponds to 34 days post-explosion, and 18-days after the first maximum and 6 days prior to the secondary, brighter visual maximum (Folatelli et al. 2006) or 9-days prior to the second bolometric maximum (Parrent et al. 2007).

3.1 General Spectroscopic Properties

Wang & Baade (2005), Anupama et al. (2005), Folatelli et al. (2006) and Parrent et al. (2007) have previously presented discussion of the spectroscopic properties of SN 2005bf at various epochs. Here we briefly summarise the properties of this observation of SN 2005bf, to serve as an orientation for the discussion to follow.

The flux spectrum of SN 2005bf (the bottom panel of Fig. 2) is dominated by a series of broad P Cygni profiles, with several features attributable to He. The dominant He I feature is that of 5876Å, with the minimum of the absorption component at $-6\ 700\text{km s}^{-1}$. It is noted, however, that the emission component of the He I 5876Å P Cygni profile is not centred on the rest wavelength, rather it is displaced blueward by $\sim 1\ 500\text{km s}^{-1}$. The emission components of the He I 5016,6678,7065Å lines are similarly blue shifted, with similar absorption velocities as the He I 5876Å line.

At the blue extreme of the spectrum Ca II H&K are clearly visible as a single profile, and a P Cygni absorption associated with the Ca II IR triplet is visible at the red extreme of the spectrum. The single Ca II H&K absorption corresponds to an average velocity of $-11\ 700\text{km s}^{-1}$, and the IR triplet absorption minimum corresponds to a velocity of $\sim -12\ 500\text{km s}^{-1}$. A series of Fe II lines are observed as P Cygni profiles and

identified, following Anupama et al. (2005), as: lines 4520, 4549, 4584, 4629Å (multiplets 37 and 38) as a single P Cygni profile and 4924, 5015, 5169Å (multiplet 42). The absorption minima correspond to expansion velocities of $-7\ 700\text{km s}^{-1}$.

Despite classification as a Type Ic SNe, Wang & Baade (2005) and Parrent et al. (2007) have identified possible High Velocity (HV) components of hydrogen H α , H β and H γ at $-15\ 000\text{km s}^{-1}$. H β appears as the only unambiguous Balmer feature, superimposed on the Fe II (37,38) emission component. H α and H γ are possibly blended with Si II 6355Å and Fe II 4233Å at the photospheric expansion velocity (as defined by the velocities measured for He and Fe II lines; Wang & Baade 2005; Anupama et al. 2005; Tominaga et al. 2005; Folatelli et al. 2006; Parrent et al. 2007). Higher Balmer features are not observed due to the strong Ca II H&K feature and fading response of FORS1 at bluer wavelengths.

Weak and narrow interstellar absorptions of Ca II H&K and Na I D are observed at the recessional velocity of the host galaxy. There are no comparable absorptions for Milky Way interstellar absorption and, given the resolution of the observations and the high recessional velocity of the host galaxy, such components would be resolved if present. Schlegel et al. (1998) give the fore-ground Galactic reddening at $E(B - V) = 0.01$. The equivalent width of the Na I D line was measured, through fitting a Gaussian line profile, as $W_\lambda(\text{Na ID}) = 0.7 \pm 0.1\text{Å}$. Using the relations of Turatto et al. (2003), this corresponds to a reddening of $E(B - V) < 0.37$.

3.2 General Spectropolarimetric Properties

The polarization properties of SN 2005bf are shown in the top four panels of Fig. 2. The polarization p shows a significant gradient across the observed wavelength range, with higher polarization at the blue end of the spectrum and a decreasing level of polarization at longer wavelengths.

The polarization of the strong lines observed in the flux spectrum exhibits “inverted P-Cygni” profiles, with the polarization peaking at absorption minimum and depolarization over the emission component. High levels of polarization can be seen to be associated with Ca II H&K (peaking at $\sim 4.5\%$), Fe II lines, He I 5876Å (2.5%) and the absorption of the Ca II IR triplet (peaking at 5%, although the feature is only observed at a low S/N). This is in contrast to the weak polarization observed at H γ . The Fe II absorption at 4410Å (Wang et al. 2003; Branch et al. 2006) shows only a slight increase in $\Delta p \sim 0.3\%$ compared to background levels of polarization. There is no significant polarization associated with O I 7774Å, above the background level of polarization.

The polarization angle θ rotates as it passes over the absorption features; changing by $+20^\circ$ at the Ca II H&K absorption and -30° for He I 5876Å. The polarization angle is, however, generally constant at $\theta = 158.3 \pm 0.1$ away from conspicuous polarization associated with spectral lines. The consequence of the consistency of the polarization angle θ is evident on Fig. 3, which shows that the Q and U data fall along a dominant axis on the $Q - U$ plane. The only significant deviations from the dominant axis are across the absorption and emission features associated with P Cygni profiles, which have components along an axis orthogonal

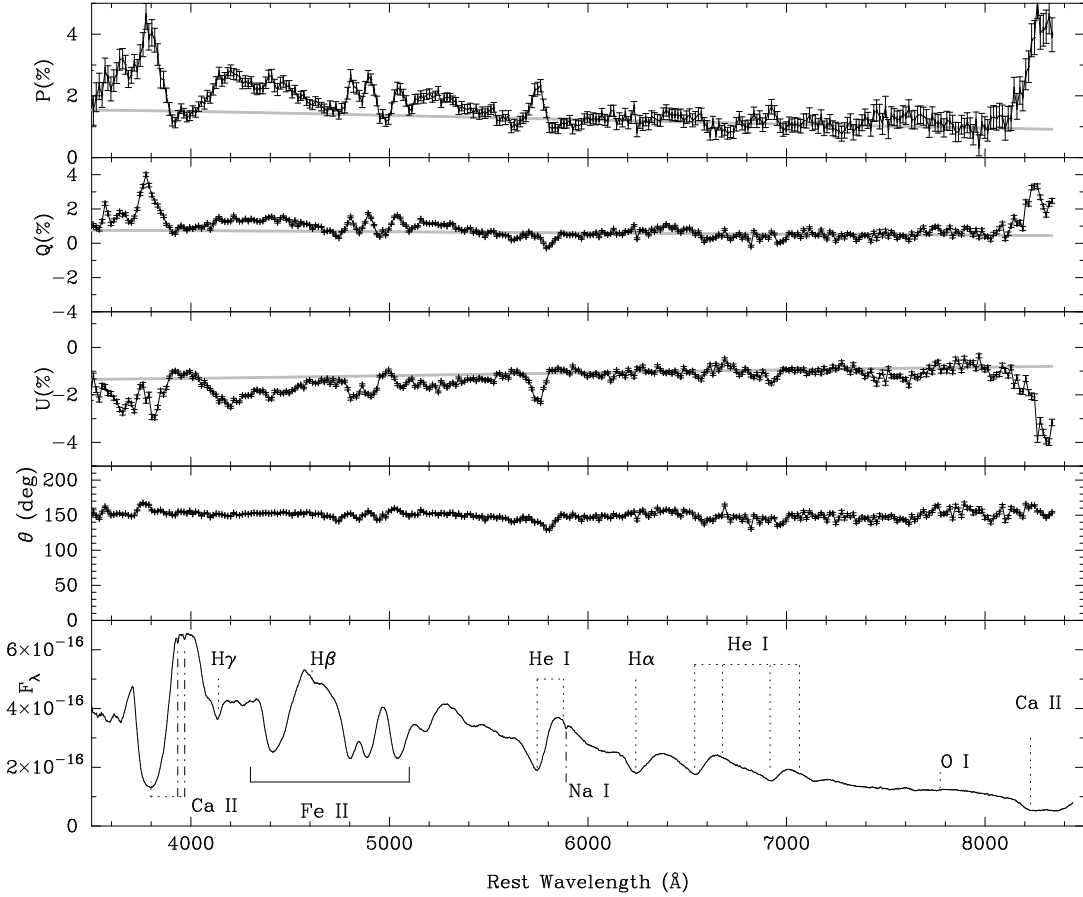


Figure 2. Spectropolarimetric observation of SN 2005bf, from 2005 Apr 30.9. The observation was conducted using ESO VLT FORS1. The panels show (from top to bottom) the polarization p , Q Stokes parameter, U Stokes parameter, the polarization angle θ and the total flux spectrum ($\text{ergs s}^{-1} \text{cm}^{-2} \text{\AA}^{-1}$). The wavelength scale of the data has been corrected for the recessional velocity of the host galaxy. The polarization parameters have been re-binned to 15\AA , while the flux spectrum is at 2.6\AA bin^{-1} . The light smooth lines are best fits for a Serkowski law-type Interstellar Polarization, for $p_{max}(ISP) = 1.6\%$, $\theta_{ISP} = 149.7^\circ$ and $\lambda_{max}(ISP) = 3000 \text{\AA}$. Dotted lines, in the bottom panel, indicate spectral features intrinsic to the SN, and dot-dashed lines indicate lines arising from the ISM in the host galaxy.

to the dominant axis on the $Q - U$ plane. The significant polarization ($\sim 1\%$) observed across depolarizing emission lines is suggestive that there is high degree of non-intrinsic polarization, with the gradient across the wavelength range being consistent with a Serkowski et al. (1975) interstellar polarization (ISP) law. The determination of the ISP is presented in Section 4.1.

4 ANALYSIS

4.1 Interstellar Polarization

The removal of the ISP is an important step in directly measuring the intrinsic polarization properties of SNe from the observed data. Wang et al. (2003) discuss three considerations for determining the ISP directly from SN observations: 1) Assume that the emission lines are completely depolarized; 2) Assume the ISP is an unvarying polarization component between different epochs in the SN evolution; and 3) assume that observations of the SNe at the nebular phase are intrinsically unpolarized due the low density of scattering particles. In the case of this observation of SN 2005bf

the last two points are invalid, since there is only one observation at one epoch (so that a time invariant component cannot be identified) and the SN is clearly not in the nebular phase. The removal of the ISP from our observation of SN 2005bf relies, therefore, on a number of assumptions and being able to place useful limits of the size of the ISP.

Limits on the degree of polarization can be set by considering the amount of reddening along the line of sight and the relation between reddening and the degree of the ISP. Serkowski et al. (1975) find that $p_{ISP}(\%) < 9E(B-V)$, such that reddening places a maximum limit on the value of the ISP. For the three reddenings determined in Section 3, we find the $p_{ISP} < 0.09\%$, for Galactic foreground reddening, and 3.3% , for internal reddening in the host as measured by the Na I D line. These maximum limits are presented, on the $Q - U$ plane, on Fig. 3. The majority of the reddening of SN 2005bf arises in the host galaxy, as the only Na I D component observed is at the redshift of the host. In addition, in the catalogue of Heiles (2000)⁴ there are two polarized Galactic stars, HD 90994 and 92886, which lie within 5° of

⁴ Referenced using Vizier - <http://vizier.u-strasbg.fr/>

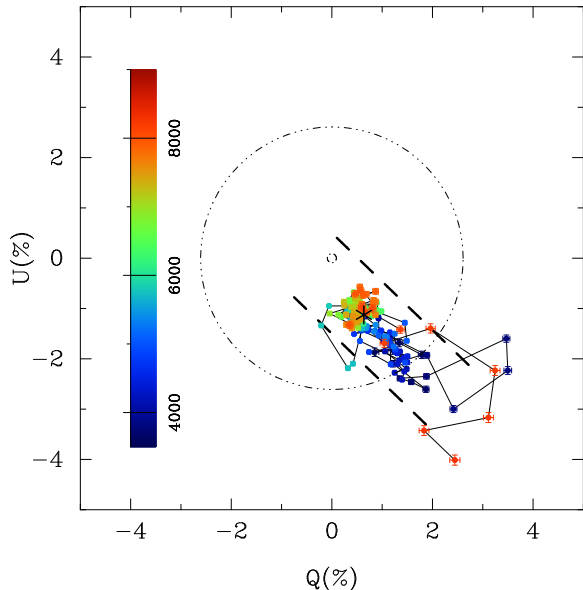


Figure 3. Spectropolarimetric observation of 2005bf plotted on the $Q-U$ plane. The points are colour coded according to their wavelengths following the scheme of the colour bar on the left hand side of the figure, and the data have been re-binned to 30\AA . The data are distributed along a preferred axis, between the two heavy dashed lines (which indicate the approximate extent of the data on the $Q-U$ plane, and are parallel to the dominant axis uncorrected for the ISP). The limits on the ISP, as determined from reddening considerations, are shown as circles for a) *inner circle* Galactic reddening $E(B-V) = 0.01$ and $p < 0.09\%$ and b) *outer circle* host reddening $E(B-V) = 0.37$ and $p < 3.3\%$. The location of the determined ISP component (see §4.1), at 5500\AA , is indicated by asterisk.

SN 2005bf on the sky. Both of these stars are at a Galactic Latitude of $b = 46^\circ$ and distances $< 460\text{pc}$, and have polarizations $< 0.1\%$ suggesting only a small Milky Way contribution to the ISP. The Serkowski et al. (1975) relation only provides an upper limits on p_{ISP} , which only serves to provide a guide for more direct techniques which aim to determine the ISP directly from the observations of the SN itself.

We note from Fig. 2 that the emission features of Ca II H&K, the Fe II lines from $4900\text{-}5300\text{\AA}$ and the He I 5876\AA line display significantly lower polarizations than either the associated absorption features (McCall 1984) or the continuum in the immediate vicinity. This suggests that there is a high level of intrinsic polarization to the SN, but that, even for features that are expected to be completely depolarized, the ISP is $\sim 1\%$. Because of the relatively high level of SN polarization, with respect to the ISP, a single vectorial subtraction of constant values of Q_{ISP} and U_{ISP} at every wavelength is inappropriate. Instead, it is required that the ISP be calculated at each wavelength, according to a Serkowski et al. (1975) law, where:

$$p(\lambda) = p_{max} \exp(-K \ln^2(\lambda_{max}/\lambda)) \quad (1)$$

where Whittet et al. (1992) give:

$$K = 0.01 + 1.66\lambda_{max}(\mu\text{m}) \quad (2)$$

The calculation of the corresponding Stokes parameters $Q_{ISP}(\lambda)$ and $U_{ISP}(\lambda)$ requires the assumption of a constant polarization angle and, hence, that $Q_{ISP}(\lambda)$ and $U_{ISP}(\lambda)$ are in the same ratio across the wavelength range. In addition, the ISP can be located on the $Q-U$ plane by demanding that it lie along the dominant axis of the observed data (Wang et al. 2003). In the case of SN 2005bf such a dominant axis is observed, and the ISP can be located at either end of distribution of the data on the $Q-U$ plane. Given the high density of depolarizing resonance lines at the blue end of the spectrum, it is expected that the ISP is located on the $Q-U$ plane closest to the bluest data along the dominant axis (Howell et al. 2001). The polarization angle associated with the depolarizing emission lines is measured as $\theta_{ISP} = 149.7^\circ \pm 4.0$ (see Fig. 3). This result is surprising, since there is an expectation that the ISP should be aligned with the spiral arms of the host galaxy, as shown as Fig. 1 (Scarrott et al. 1987). SN 2005bf is, however, significantly displaced from the nearest spiral arm and the case, therefore, for the polarization angle of the ISP is not expected be as straightforward as the cases of SN 2001ig (Maund et al. 2007) or SN 2006X (Patat et al. 2007). The validity of the assumption used here to calculate the ISP is discussed in §5.4.

A simultaneous χ^2 -fit of a Serkowski et al. ISP law (of the functional form given in Eqn. 1), for the parameters p_{max} and λ_{max} , was conducted using the narrow wavelength regions corresponding to the minimum degrees of polarization, at the peaks of the emission lines in the flux spectrum. The χ^2 minimization was conducted for the polarization p and the two Stokes parameters Q and U . In this way the value of the polarization angle of the ISP could also be tested, since χ^2 should be minimized for the same values p_{max} and λ_{max} for independent fits to p , Q and U , if θ_{ISP} is correct. Statistically significant values of χ^2 and simultaneous minima in the $\lambda_{max} - p_{max}$ plane were only achieved for values of $\theta_{ISP} = 149.7^\circ \pm 4.0$. This demonstrates that our value of the polarization angle of the ISP is consistent with our assumption that the Fe II lines are depolarized. There is a certain degree of degeneracy between p_{max} and λ_{max} , but the rising degree of polarization observed at the emission lines suggested that the polarization was increasing blueward and that λ_{max} was located blueward of the observed data. The best-fit values were $p_{max} = 1.6 \pm 0.2\%$ (99% confidence) at $\lambda_{max} = 3000\text{\AA}$.

The ISP and the Stokes parameters $Q_{ISP}(\lambda)$ and $U_{ISP}(\lambda)$ are shown on Fig. 2. The subtraction of the wavelength-dependent ISP, shown on the $Q-U$ plane as Fig. 4, contracts the data about the origin, except for the polarization associated with certain lines. The degree of the ISP across the B and V photometric bands ($\sim 1.5\%$) conversely limits the amount of reddening along the line of sight to $E(B-V) > 0.17$.

The values of λ_{max} determined here is substantially bluer than that measured by Serkowski et al. (1975) for Galactic stars. Patat et al. (2007) found a similar value of λ_{max} was applicable for the ISP for SN 2006X; however, in that case the wavelength dependence of the ISP did not conform to a standard Galactic Serkowski et al.-type law or a value of K consistent with Whittet et al. (1992).

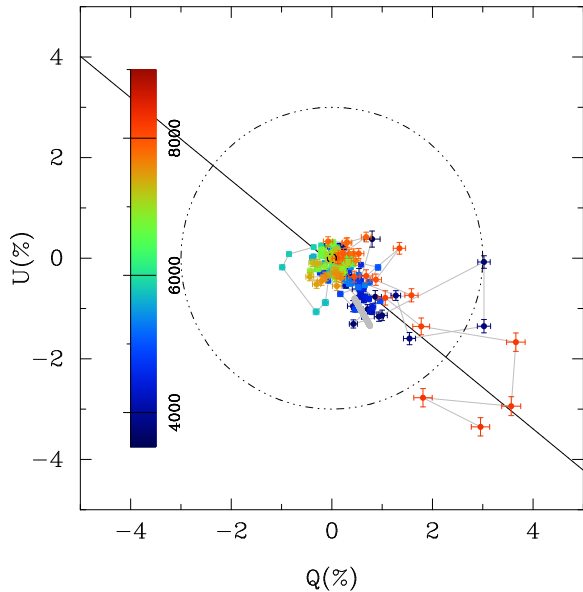


Figure 4. Spectropolarimetric observation of SN 2005bf plotted on the $Q - U$ plane, with the determined wavelength-dependent ISP subtracted. The dominant axis of the data is indicated by the straight line. The points are colour coded according to their wavelengths following the scheme of the colour bar on the left hand side of the figure, and the data have been re-binned to 30\AA . The wavelength dependent ISP is indicated by the grey line. The He I 5876\AA , Ca II H&K and Ca II IR Triplet are seen to significantly deviate, in the form of loops, from the central concentration of data within $p < 0.45\%$ of the origin.

4.2 Intrinsic Polarization

After the subtraction of the ISP, significant polarization is still observed across the spectrum, particularly associated with spectral lines. Given the shallow wavelength-dependence of Eqn. 1 the ISP can, potentially, remove some intrinsic polarization from the data but cannot remove polarization associated with spectral features that vary widely over short wavelength ranges. Specific polarization features are discussed at length in the following sections. There appears to be a degree of “continuum” polarization, for regions of the spectrum over which the Stokes parameters hardly vary. This is the case for data in the range $6000 < \lambda < 8000\text{\AA}$, where the average polarization is 0.45% , but shows no apparent correlation with features in the flux spectrum. The bulk of the data, on the $Q - U$ plane (see Fig. 4), lies within $p \approx 0.45\%$ of the origin, with the obvious exceptions of He I and Ca II lines. This degree of polarization implies asymmetries of the order $\gtrsim 10\%$ (Höflich 1991).

4.3 He I 5876\AA

As discussed previously, the He I 5876\AA line shows a significant degree of polarization, rising from a continuum level of 0.2% to 1.3% at the absorption minimum. The emission component, after ISP subtraction, has no polarization, as assumed in the calculation of the ISP presented in Sec. 4.1. The increase in polarization, anti-correlated with the flux spectrum of the absorption line, is matched by a rotation in the polarization angle corresponding to 0° at the continuum

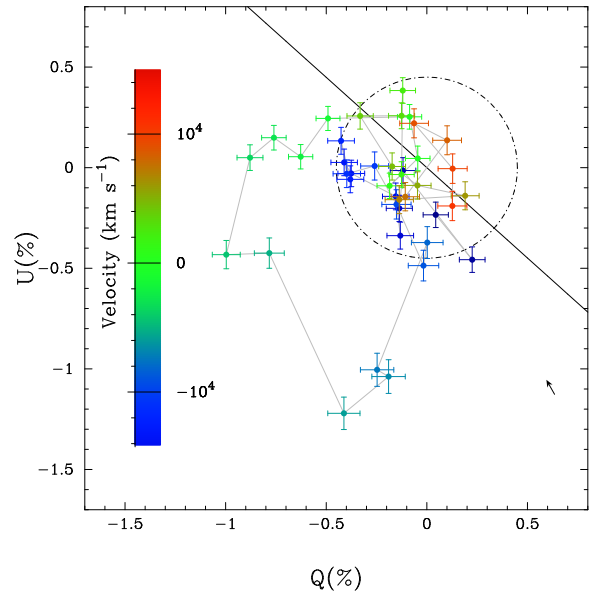


Figure 5. The Q and U Stokes parameters around the He I 5876\AA line. The data have been re-binned to 15\AA (or 765km s^{-1} at 5876\AA). The points are colour coded by the observed velocity (km s^{-1}) relative to the rest wavelength of the line. The dominant axis, determined for the entire data set as shown in Fig. 4, is shown as the straight black line. The arrow indicates the degree of ISP which, due to wavelength dependence, shows the degree of ISP from blue to red wavelengths. The dot-dashed circle shows the region of “continuum” polarization $p = 0.45\%$.

level to 50° at the line centre. This corresponds to the production of a loop, as seen on Figs. 3, 4 and, specifically, 5. The effect of the ISP, and in particular its orientation, stretches the loop in the direction of the ISP angle and away from the origin of the $Q - U$ plane. While the subtraction of the ISP causes the loop to be contracted, it is still clear that the loop structure, on the $Q - U$ plane, is intrinsic to the SN itself.

The loop structure, shown on Fig. 5, lies on only one side of the dominant axis, and the emission component can be seen to lie at the origin of the $Q - U$ plane, since it is measured to be completely depolarized. The bulk of the loop structure is formed by wavelengths blueward of the rest wavelength of this line.

In this case, a simple straight-line fit to data on the $Q - U$ plane (see Wang et al. 2006) would yield only a poor fit, since it is clear that the structure is a loop. There is no rotational transformation on the $Q - U$ plane, to rotate the parameters to “dominant” and “orthogonal” axes, that can remove the loop (Maund et al. 2007).

4.4 Ca II H&K and IR Triplet

The highest degrees of polarization, across the observed spectral range, are measured for the Ca II H&K and IR triplet as $2.9 \pm 0.7\%$ and $4 \pm 1\%$, respectively. On the $Q - U$ plane, as plotted in Fig. 4, the Stokes parameters across these two lines are observed to occupy approximately the same area with the same orientation relative to the origin. A relatively high degree of uncertainty on these values is caused by low levels of signal-to-noise at these wavelengths,

due to the limited response of FORS1 at both the blue and red extremes of the data. Even so, the degrees of polarization associated with these features are still significantly higher than for any other features in the spectrum.

Whereas the He I 5876Å line rotated by 50°, as discussed in Section 4.3, a different amount of rotation of the polarization angle is observed across these features (from 60 through 85°) is observed; although in the case of the Ca II IR triplet the data is incomplete as the emission component lies redward of the spectral range of the observation. Furthermore, the $Q - U$ data associated with these features show that they are approximately aligned with the determined ISP. This leads to some concern over the veracity of the measured value of the polarization angle across these features. The amount by which the polarization angle rotates across the lines should not be affected, since that is a relative change. Again, this problem is most likely due to uncertainties in the Stokes parameters induced by the low signal-to-noise ratio of the data at these wavelengths. These effects would also cause the Stokes Q and U parameters to deviate from the clear loop structure observed for such lines as He I 5876Å. If the Stokes parameters across these two lines are assumed to be correct then the polarization angle measured across these two lines are: 1) consistent for the two Ca lines, suggesting production of both these lines by Ca ions with the same distribution within the ejecta; and 2) that Ca has a significantly different distribution within the ejecta compared to He.

4.5 HV HI $H\alpha$, $H\beta$ and $H\gamma$

As discussed in Section 3.1, a series of absorption features in the spectrum can be identified as $H\alpha$, $H\beta$ and $H\gamma$ at high velocities. Anupama et al. (2005), Tominaga et al. (2005) and Parrent et al. (2007) debate, however, the relative contributions of H and other possibly blended species, such as Si II and Fe II. Blending with other lines, with different polarization properties, would cause differences in the observed polarizations for each of the Balmer lines. Spectropolarimetry can, therefore, be used to assess the importance of blending, when considering particular line identifications.

Small increases in the degree of polarization, across the Balmer features, are shown as Fig. 6. The peaks in polarization are seen to disagree with the absorption minima of the line profiles in the flux spectrum for $H\alpha$ and $H\gamma$, even though the minima for the three lines have similar velocities to within 1 bin (or 765km s^{-1}) in the flux spectrum.

There is no detectable loop structure associated with the HV HI features, which is to be expected given that the polarization associated with these features is low relative to the degree of the continuum polarization either side of each of these lines, in wavelength space. Instead, the principal measurable signature of these lines is the total polarization itself. The smallest degree of polarization for these possible HV features is observed for $H\beta$, where the increase in polarization over the background polarization is $0.1 \pm 0.1\%$. The low degree of polarization might have two possible causes: 1) the superposition of the absorption on the depolarizing Fe II (multiplet 37,38) emission component; and 2) the low optical depth which would give rise to such weak absorption features in the flux spectrum. This is at odds with higher degrees of polarization associated with $H\alpha$ and $H\gamma$. As dis-

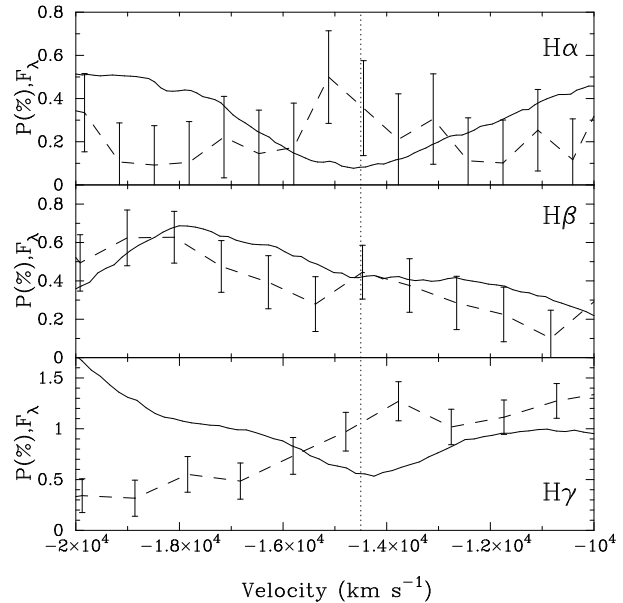


Figure 6. The polarization across the high-velocity HI Balmer absorption lines, as a function of velocity. The flux spectrum, arbitrarily scaled is shown as the solid black line, with polarization measurements p shown as points with error bars and the dashed lines. The approximate central velocity for the absorption minima of all of the lines is indicated by the dotted line.

cussed above, $H\beta$ is the only Balmer line not associated with possible absorption features due to other species, leading to $H\beta$ being effectively the “cleanest” Balmer absorption.

If homologous expansion is assumed, then the HV H I components are exterior to the slower moving Fe II lines, which implies that the depolarized photons of Fe II are repolarized purely by $H\beta$. As presented in Sec. 3.1, $H\alpha$ and $H\gamma$ may be contaminated by Si II 6355Å and Fe II 4233Å moving at only the photospheric velocity. Certainly in the case of the Fe II line there are other comparison lines, discussed in Sec. 4.6, which do show significant polarization associated with their absorption features. It is more likely, perhaps, that the polarization signature observed for $H\alpha$ and $H\gamma$ arises from blends of the Si and Fe lines. The polarization of the $H\gamma$ line is identical to other Fe II lines, in the degree of polarization and the amount through which it rotates across the absorption profile. This indicates that Fe II 4233Å is likely to be responsible for most of the observed polarization for this feature. The degree of polarization intrinsic to the H I lines themselves can, therefore, be limited by the amount observed for $H\beta$ to $p(\text{HI}) \lesssim 0.2\%$. The observation of any polarization associated with the HV Balmer series is surprising, since the weakness of these lines suggests low densities in the HV shells which would lead to only a small amount of polarization actually associated with these lines.

4.6 Fe lines

The difference in the polarization properties of the Fe II lines of multiplets 37,38; and 42 can be viewed as primarily due to line blending effects. The close proximity of the Fe II lines of multiplets 37,38 (in wavelength space) leads to the production of a single P Cygni profile, but results in only

a small increase ($\sim 0.3\%$) in the local level of polarization. The flux at the absorptions associated with the redder lines of these two multiplets are dominated by the depolarized flux from the emission of the bluer lines.

For multiplet 42 there is sufficient separation of the lines to yield resolved components in the flux spectrum, with resolved peaks in the polarization spectrum. If the degree of flux associated with the absorption of the redder lines is significant, relative to the amount of depolarized flux from the emission components of the two bluest lines, there would be a significant intrinsic polarization observed at the peaks of the emission components. This would, therefore, imply that the ISP determined by the assumption of depolarization associated with these Fe lines is, in fact, an upper limit of the degree of ISP. The lack of further observations at additional epochs, however, limits the discussion of just how inappropriate this assumption, used to calculate the ISP, actually is.

Given the significant degree of polarization associated with the absorption components of the lines of Fe II multiplets 37,38 and 42, it is to be expected that significant degrees would also be associated with other Fe II lines. Anupama et al. (2005) identify the presence of Fe II $\lambda 4233$ (of multiplet 27). Given the measured velocities of the redder Fe II lines, as 7700km s^{-1} , this implies that the absorption of this Fe II line would be coincident with HV H γ at $15\,000\text{km s}^{-1}$. The increase in polarization associated with the absorption feature at $\sim 4130\text{\AA}$ is, therefore, more likely to be due to Fe II absorption. Furthermore, there is possible blending of Fe II 5169\AA with Fe III 5156\AA which cannot be resolved.

It is noted that the maximum degrees of polarization associated with Fe II lines are approximately similar ($\sim 1 - 1.5\%$), and that the Stokes Q and U parameters and the polarization angles are also similar. The Fe lines demonstrate a larger degree of rotation in the polarization angle across the absorption profiles (from 20 to 80° , from the blue wing to the absorption minimum, after correction for the ISP) than observed for either Ca and He. This suggests that the distribution of Fe is different to that of both He and Ca in the SN ejecta.

5 DISCUSSION

A number of studies have been conducted of the photometric and spectroscopic evolution of SN 2005bf. In this respect, the amount of spectropolarimetry data available for this SN is extremely low, but it is important.

The low degree of intrinsic “continuum” polarization, $< 0.45\%$, implies asymmetries of only 10% . Höflich (1991) shows that the observed polarization for an oblate ellipsoid can be reduced by inclining it to the observer. This may, indeed, be the case with SN 2005bf; there are, in any case, obvious asymmetries in SN 2005bf. A polarization of 0.45% is larger than the values of the continuum polarization reported by Wang et al. (2003) for SN 2002ap at earlier epochs. While the photosphere itself may not be highly asymmetric, it is clear from the polarization signatures associated with spectral lines that the ejecta within the line forming region are highly asymmetric (McCall 1984) and, importantly, highly stratified. Comparison of all the

different species giving rise to lines with strong polarization signatures shows they must occupy different parts of the ejecta to give rise to different polarization angles.

5.1 Loops on the Q-U plane

The presence of loop structure on the $Q - U$ plane for SN 2005bf is quite similar to that observed for SN 2002ap by Wang et al. (2003). The He I 5876\AA line of SN 2005bf may be produced by the same mechanism that Wang et al. suggested for the O I 7774\AA line in SN 2002ap: the line forming region and the continuum forming region beneath do not share the same axial symmetry and can be characterised by two different polarization angles. The varying contribution of scattered flux from the blue edge of the absorption to the absorption minimum leads to different ratios of the polarized flux from the two regions and, hence, varying polarization angle, leading to a loop on the $Q - U$ plane. In the case of a SN, this can arise from the absorption line forming region and the photosphere not having the same shape.

Loops on the $Q - U$ plane, associated with the absorption components of P Cygni profiles, were identified by Cropper et al. (1988) in observations of SN 1987A. A loop was observed for the Ca II HV component of the Type Ia SN 2001el and a series of models, including ellipsoidal shells and clumped ejecta, were found to approximately reproduce such a feature (Kasen et al. 2003). Hoffman (2006) identified loop structure in Type IIn SNe, and characterised the CSM as a series of ellipsoidal shells with varying orientations. Maund et al. (2007) identified loop-like features in spectropolarimetry of the Type IIb SN 2001ig, which were interpreted as the presence of a significant non-bipolar component of the ejecta (Höflich et al. 2001). As Kasen et al. (2003) indicate, however, the determination of the structure of the ejecta from single loops in the $Q - U$ plane is extremely difficult, requiring the computational sampling of a large amount of parameter space. While it is not clear how the loop of the He I 5876\AA line should be interpreted, it is indicative of varying symmetries in the SN ejecta rather than one major axial symmetry.

In SN 2005bf we also observe large structures on the $Q - U$ plane for Ca II H&K and the IR triplet. While the latter loop is incomplete and the data for both features suffer from poor S/N, there is a significant polarization associated with these lines. The polarization angles of these lines are at a different orientation than the He I 5876\AA line, suggesting a different distribution in the ejecta. The flux spectrum also suggests this property, with the absorption minima of both Ca lines occurring at substantially higher velocities than the photospheric velocity determined from He I and Fe II lines. Maund et al. (2007) observe similar behaviour in the Ca II IR triplet feature of SN 2001ig, where it does not share the same orientation with the rest of the data from each particular epoch. While Maund et al. suggested some possible link with the CSM-ejecta interaction, it is clear that here the Ca II component is moving much slower than the HV Balmer lines and, unlike SN 2001el (Wang et al. 2003), Ca II is not observed as two separable photospheric and HV components. Again, we suggest some caution in interpreting the polarization angle of the Ca II lines due to

possible correlation with the determined ISP.

5.2 HV Balmer Components

The HV components of the Balmer series that we observe here are consistent with the expectations that thin shells of hydrogen may remain on the massive progenitors of this type of SN. HV components are more commonly observed for the Ca II IR triplet in Type Ia SNe, but they are also observed in CCSN types as they are produced by approximately the same physics (Chugai et al. 2007). Spectropolarimetry of these features is rare, and the most direct comparison is made with Ca II HV features in Type Ia SNe. Wang et al. (2003) observed polarizations of 0.7% for SN 2001el, inferring a mass of $0.004M_{\odot}$ in the HV component. Chornock & Filippenko (2006) did not, however, see any polarization of that feature for the very similar SN 2004S. Patat et al. (2007) have observed an HV component polarization of $\sim 1.1\%$ in SN 2006X, again a similar event to SN 2001el. The upper limit on the intrinsic polarization of the H I features of SN 2005bf is substantially lower, therefore, than the polarizations measured for HV features in Type Ia SNe. The low upper limit of the amount of polarization intrinsic to H I itself and the lack of any significant deviation of the polarization angle from the background values make it unlikely that the observed polarization is coming from a geometrically distinct plane as Wang et al. (2003) observed for Ca II in SN 2001el.

5.3 SN 2005bf vs. SN 2002ap

The opportunities to conduct spectropolarimetry of CCSNe are increasing, however it is still too soon to have a complete set of observations for all of the diverse types of CCSNe. Anupama et al. (2005) state that SN 2005bf is a close relative of the peculiar Type Ib SN 1999ex; but SN 2005bf is, to the best of our knowledge, the only example of this type of SN with spectropolarimetry.

The object with the most comparable spectropolarimetry data set is SN 2002ap, which was observed by Wang et al. (2003), Leonard et al. (2002) and Kawabata et al. (2002). SN 2005bf is similar to SN 2002ap in that the Stokes parameters for the bulk of the data are concentrated around the origin of the $Q-U$ plane. Between 3 (Wang et al. 2003) and 25 days (Leonard et al. 2002) after V maximum, SN 2002ap shows lower levels of polarization ($\sim 0.3\%$) across large wavelength regions than this particular epoch of SN 2005bf. The only feature of SN 2002ap that has a distinct and significantly different polarization is O I 7774Å; this line is not observed to be significantly polarized in SN 2005bf. Similarly, at 6 days prior maximum the polarization of SN 2002ap was dominated by the O I 7774Å line, with most of the spectrum at $p \lesssim 0.25\%$. Wang et al. (2003) observed that the “continuum” polarization of SN 2002ap increased with age, become less concentrated around the origin of the $Q-U$ plane.

For SN 2005bf we observe that there are a number of features that are significantly more polarized than the

continuum polarization, most notably the Ca II lines and He I 5876Å; but also that the Stokes parameters of the data at the “continuum” are less concentrated about the origin of the $Q-U$ plane (within a radius of $p = 0.45\%$) than Wang et al. (2003) observed for SN 2002ap at early times. A re-reduction of the entire Wang et al. data set was conducted, to test whether the scatter of the data on the $Q-U$ plane might have been due to a numerical effect in our new data reduction routines. The result of this additional test was a complete set of Stokes parameters for all of the observations of SN 2002ap which were completely consistent with the results presented by Wang et al.. This demonstrates that our new routines would have been able to easily resolve the structure measured for SN 2002ap, and the scatter observed for the data of SN 2005bf is, in fact, real and not due to the new routines.

5.4 Estimate of the ISP

There are a number of limitations to the conclusions that can be drawn about the geometry of SN 2005bf, given that there is only an observation at a single epoch. There were multiple observations of SN 2002ap by Wang et al. (2003), Leonard et al. (2002) and Kawabata et al. (2002). The benefit from having data from multiple epochs is clear, especially by being able to follow the evolution of particular features.

Additional observations could provide a direct measure of the ISP, by determining the non-varying polarization component, due to the ISP, present at each epoch. The determination of the ISP presented here is based on an assumption that emission lines are completely depolarized. Given the degree of potential blending of the Fe II lines, discussed in Sec 4.6, it is possible that the emission lines are *not* completely depolarized, in which case the determined ISP overestimates the real value of the ISP (Tran et al. 1997).

If the degree of the ISP is lower than determined here, then the degree of the measured continuum polarization would be higher leading to a higher degree of inferred asymmetry. The slight wavelength-dependence of the ISP, however, would lead to less contraction of the data about the origin of the $Q-U$ plane; since continuum polarization would be higher at the blue end of the spectrum causing the data to be farther from the origin of the $Q-U$ plane than the data at the red end of the spectrum. The measured Stokes parameters of the spectral lines would, however, remain almost unchanged, since the polarization varies over these spectral lines on significantly smaller wavelength scales than the ISP. The polarization measured for the spectral lines and the conclusions drawn from them are, therefore, very real. There is concern about the measured polarization angle of the Ca features and the similarity of these angles with the ISP; further spectropolarimetry of SN 2005bf at other epochs would have revealed if this is, indeed, merely coincidence. If the other extreme of the ISP is considered, whereby all of the polarization is intrinsic to the SN, this would only imply asymmetries of the order 20%.

5.5 Comparison with Two-Component Explosion Models

Tominaga et al. (2005) and Folatelli et al. (2006) presented two distinct models to explain the spectroscopic evolution of SN 2005bf. Folatelli et al. (2006) presented a two-component model with the first, polar, component dominating the spectra and light curve at earlier epochs with the signature of a Type Ic SN, followed by a lower velocity, more isotropic component containing most of the He. Tominaga et al. (2005) suggest that the emergence of He in the spectrum was due to growth of “holes” in the ejecta, as it expanded, permitting gamma rays to be deposited into the He envelope leading to the excitation of He at later epochs.

Some polarization of the He absorption feature may arise from the recombination front of He just outside the photosphere, in this case the inferred asymmetry would be consistent with that of the photosphere. It is clear, however, that the observed polarization of the He lines, and the inferred asymmetry, is dominated by the excited He component that is not coupled to the asymmetry of the photosphere.

It is clear, however, from studies such as Tominaga et al. (2005) and Folatelli et al. (2006) that SN 2005bf was not, at earlier epochs, a “classical” Type Ic SN (see Wheeler & Benetti 2000). As mentioned above, the weak O I 7774Å line with no discernible associated polarization is in stark contrast to Type Ic SNe such as SN 2002ap. This suggests that the C-O core is still shielded by the photosphere, which is located within the He envelope. The weakness of the line and the lack of polarization all indicate that the line is formed by primordial O I in the He envelope.

The absence of peculiarly strong iron features, with strong polarization signatures and substantially different polarization angles compared to He and Ca, seems to suggest that jet structure, originating from the core, is not present. This is in agreement with the lack of a highly polarized O I feature, that would be expected if core material were brought to the photosphere by a jet. In addition, the orientation of the polarization angles of the He I and Ca II features, along with the presence of low polarization HV H I components, suggest the explosion of an He star. It seems unlikely, therefore, that a jet penetrated the surface of the star. We suggest that the excitation of He I and Ca II is more likely due to an asymmetric Ni distribution (perhaps due to a jet that stalled inside the progenitor) that only at later epochs, due to decreasing optical depth with the expansion of the SN, deposited energy directly into the He envelope to produce He features and cause the transition from a Type Ic to a Type Ib SN. The spectropolarimetry data, therefore, favours the model proposed by Tominaga et al. (2005), but with the specific interpretation that the “holes” are due to partial penetration of the He envelope by a Ni-rich jet, reminiscent of Folatelli et al. (2006).

This model is presented as Fig. 7.

Additional spectropolarimetry observations at earlier epochs, in comparison with the observation at this epoch, could have potentially directly distinguished between these two models. The presence of a jet, following the model of Folatelli et al. (2006), would have had polarization characteristics clearly distinct from that observed at this epoch. Indeed, given the highly asymmetric nature of a jet, the high level of polarization at earlier times may have followed

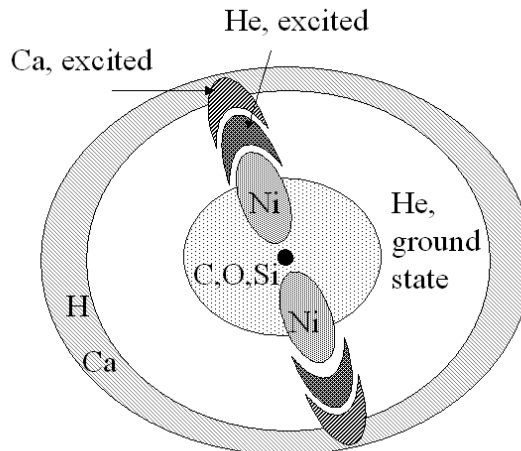


Figure 7. A schematic of the structure of SN 2005bf, based on the spectropolarimetry presented here and the models of Tominaga et al. (2005) and Folatelli et al. (2006). The observed polarization of He and Ca lines are due to asymmetric excitation of these elements, due to asymmetric distributions of Ni and, hence, gamma-ray deposition. The continuum polarization arises from the asymmetry of the photosphere. The Ni jet axis is misaligned compared to the axis of the photosphere. Loops on the $Q-U$ plane for He and Ca lines are produced by the different orientations of asymmetries of these elements and the photosphere. Core-material and products of nucleosynthesis are shielded by the photosphere. The photosphere is immediately exterior to the C-O core, but is located inside the He-envelope. He exterior to the photosphere is unexcited.

similar behaviour as that observed for the Type Ic SN 1997X up to 15 days post-explosion (Wang et al. 2001).

6 CONCLUSIONS

A single epoch of spectropolarimetry of SN 2005bf, on 2005 Apr 30.9 and 9 days prior to second B light curve maximum, show significant polarization. There is a strong polarization component due to the intervening interstellar medium in the host, corresponding to a Serkowski law with $p_{max} = 1.6\%$, $\lambda_{max} = 3000\text{Å}$ with $\theta_{ISP} = 149.7 \pm 4.0$. This limits the reddening towards SN 2005bf to $E(B - V) > 0.17$. Possible blending effects of multiple Fe II lines may cause this estimate to be an upper limit on the ISP.

After subtraction of the ISP component, SN 2005bf is revealed to still be strongly polarized in the continuum consistent with a physical asymmetry of $\sim 10\%$.

Even larger polarization and asymmetry is correlated with spectral features. The Ca II H&K and IR triplet absorption features show the highest degrees of polarization. The polarization angles, and the rotation of the polarization angle across the line profiles, are the same. Caution is recommended about interpreting the absolute offset of the polarization angles of these lines, since these lines were observed at the limits of the FORS1 response function.

Significant polarization is observed across the He I 5876Å line, peaking at 1.1% above the background polarization.

The rotation of the polarization angle across the He I feature yielded a loop on the $Q-U$ plane, but the polarization angles observed for He I 5876Å were not aligned with those observed for the absorptions of the two Ca lines. The High Velocity H I lines are observed, with $H\beta$ being the least blended. Significant increases in polarization across the profiles of $H\alpha$ and $H\gamma$ are suggested as most likely being due to blends with the polarized absorption components of Si II 6355Å and Fe II 4233Å, moving at the slower photospheric velocity. The slight detection of any polarization at HV $H\beta$, superimposed on a depolarizing Fe II line emission component, is proposed as evidence that the features due to hydrogen are not significantly polarized themselves to within $p(HI) \lesssim 0.2\%$. This is most likely due to the HV component being a low mass shell of H I and, hence, with low optical depth.

Spectral features of Fe II and O I are observed to be neither particularly strong nor excessively polarized, suggesting they arose in the He envelope and were not asymmetrically deposited by a jet penetrating the envelope. The polarization of He I and Ca II absorption features is due to increased deposition of gamma-rays from Ni, due to the decrease in the optical depth to these gamma-rays with the expansion of the SN ejecta. A “tilted-jet” model may account for the array of polarization features.

ACKNOWLEDGEMENTS

The authors are grateful to the European Southern Observatory for the generous allocation of observing time. They especially thank the staff of the Paranal Observatory for their competent and never-tiring support of this project in service mode. The research of JRM and JCW is supported in part by NSF grant AST-0406740 and NASA grant NNG04GL00G.

References

- Anupama G. C., Sahu D. K., Deng J., Nomoto K., Tominaga N., Tanaka M., Mazzali P. A., Prabhu T. P., 2005, *ApJL*, 631, L125
- Appenzeller I., Fricke K., Furtig W., Gassler W., Hafner R., Harkl R., Hess H.-J., Hummel W., et al. 1998, *The Messenger*, 94, 1
- Branch D., Jeffery D. J., Young T. R., Baron E., 2006, *PASP*, 118, 791
- Chornock R., Filippenko A. V., 2006, *ArXiv Astrophysics e-prints*
- Chugai N. N., Chevalier R. A., Utrobin V. P., 2007, *ArXiv Astrophysics e-prints*
- Cropper M., Bailey J., McCowage J., Cannon R. D., Couch W. J., 1988, *MNRAS*, 231, 695
- Dray L. M., Dale J. E., Beer M. E., Napiwotzki R., King A. R., 2005, *MNRAS*, 364, 59
- Fesen R. A., Hammell M. C., Morse J., Chevalier R. A., Borkowski K. J., Dopita M. A., Gerardy C. L., Lawrence S. S., Raymond J. C., van den Bergh S., 2006, *ApJ*, 645, 283
- Filippenko A. V., 1997, *ARAA*, 35, 309
- Folatelli G., Contreras C., Phillips M. M., Woosley S. E., Blinnikov S., Morrell N., Suntzeff N. B., Lee B. L., et al., 2006, *ApJ*, 641, 1039
- Hamuy M., Pinto P. A., 2002, *ApJL*, 566, L63
- Heiles C., 2000, *AJ*, 119, 923
- Hoffman J. L., 2006, *ArXiv Astrophysics e-prints*
- Höflich P., 1991, *A&A*, 246, 481
- Höflich P., Khokhlov A., Wang L., 2001, in Wheeler J. C., Martel H., eds, 20th Texas Symposium on relativistic astrophysics Vol. 586 of American Institute of Physics Conference Series, Aspherical Supernova Explosions: Hydrodynamics, Radiation Transport and Observational Consequences (Plenary Talk). pp 459
- Howell D. A., Höflich P., Wang L., Wheeler J. C., 2001, *ApJ*, 556, 302
- Jehin E., O’Brien K., Szeifert T., 2005, *FORS1+2 User Manual*. ESO, Garching, 3.1 edn
- Kasen D., Nugent P., Wang L., Howell D. A., Wheeler J. C., Höflich P., Baade D., Baron E., Hauschildt P. H., 2003, *ApJ*, 593, 788
- Kawabata K. S., Jeffery D. J., Iye M., Ohshima Y., Kosugi G., Kashikawa N., Ebizuka N., et al. 2002, *ApJL*, 580, L39
- Leonard D. C., Filippenko A. V., Ardila D. R., Brotherton M. S., 2001, *ApJ*, 553, 861
- Leonard D. C., Filippenko A. V., Chornock R., Foley R. J., 2002, *PASP*, 114, 1333
- Leonard D. C., Filippenko A. V., Ganeshalingam M., Serduke F. J. D., Li W., Swift B. J., Gal-Yam A., Foley R. J., Fox D. B., Park S., Hoffman J. L., Wong D. S., 2006, *Nature*, 440, 505
- Maund J., Patat F., Baade D., Höflich P., Wang L., Wheeler J., 2007, *ApJ*, Submitted
- Mazzali P. A., Kawabata K. S., Maeda K., Nomoto K., Filippenko A. V., Ramirez-Ruiz E., Benetti S., Pian E., Deng J., Tominaga N., Ohshima Y., Iye M., Foley R. J., Matheson T., Wang L., Gal-Yam A., 2005, *Science*, 308, 1284
- McCall M. L., 1984, *MNRAS*, 210, 829
- Modjaz M., Kirshner R., Challis P., Matheson T., Landt H., 2005, *IAUC*, 8509, 3
- Monard L. A. G., Moore M., Li W., 2005, *IAUC*, 8507, 1
- Morrell N., Hamuy M., Folatelli G., Contreras C., 2005, *IAUC*, 8509, 2
- Parrent J., Branch D., Troxel M. A., Casebeer D., Jeffery D. J., Ketchum W., Baron E., Serduke F. J. D., Filippenko A. V., 2007, *PASP*, 119, 135
- Patat F., Baade D., Höflich P. A., Maund J. R., Wang L., Wheeler J. C., 2007, *A&A*
- Patat F., Romaniello M., 2006, *PASP*, 118, 146
- Scarrott S. M., Ward-Thompson D., Warren-Smith R. F., 1987, *MNRAS*, 224, 299
- Schlegel D. J., Finkbeiner D. P., Davis M., 1998, *ApJ*, 500, 525
- Serkowski K., Mathewson D. L., Ford V. L., 1975, *ApJ*, 196, 261
- Shapiro, P. R., & Sutherland, P. G. 1982, *ApJ*, 263, 902
- Tominaga N., Tanaka M., Nomoto K., Mazzali P. A., Deng J., Maeda K., Umeda H., et al., 2005, *ApJL*, 633, L97
- Tran, H. D., Filippenko, A. V., Schmidt, G. D., Bjorkman, K. S., Jannuzi, B. T., & Smith, P. S. 1997, *PASP*, 109, 489

- Turatto M., Benetti S., Cappellaro E., 2003, in Hillebrandt W., Leibundgut B., eds, *From Twilight to Highlight: The Physics of Supernovae Variety in Supernovae*. p. 200
- Wang L., Baade D., 2005, *IAUC*, 8521, 2
- Wang L., Baade D., Höflich P., Khokhlov A., Wheeler J. C., Kasen D., Nugent P. E., et al. 2003, *ApJ*, 591, 1110
- Wang L., Baade D., Höflich P., Wheeler J. C., 2003, *ApJ*, 592, 457
- Wang L., Baade D., Höflich P., Wheeler J. C., Kawabata K., Khokhlov A., Nomoto K., Patat F., 2006, *ApJ*, 653, 490
- Wang L., Howell D. A., Höflich P., Wheeler J. C., 2001, *ApJ*, 550, 1030
- Wheeler J. C., Benetti S., 2000, in Cox A. N., ed., , *Allen's Astrophysical Quantities*, 4 edn, AIP, New York
- Whittet D. C. B., Martin P. G., Hough J. H., Rouse M. F., Bailey J. A., Axon D. J., 1992, *ApJ*, 386, 562
- Woolley S. E., Bloom J. S., 2006, *ARAA*, 44, 507

This figure "2005bf_pos.jpg" is available in "jpg" format from:

<http://arxiv.org/ps/0707.2237v1>